Available online at www.sciencedirect.com
ScienceDirect
Journal of Sound and Vibration 319 (2009) 668–680
JOURNAL OF SOUND AND VIBRATION
www.elsevier.com/locate/jsvi

Free vibration of super elliptical plates with constant and variable thickness by Ritz method

Seyit Çeribaşı*, Gülay Altay

Faculty of Engineering, Bogazici University, Bebek, 34342 Istanbul, Turkey

Received 10 October 2007; received in revised form 19 April 2008; accepted 11 June 2008
Handling Editor: C.L. Morfey
Available online 11 July 2008

Abstract

In this study free vibration of simply supported and clamped super elliptical plates is investigated. This class of plates includes a wide range of external boundaries varying from an ellipse to a rectangle. Although studies on the upper and lower bounds of these plate geometries, namely circle and rectangle, are quite extensive, contributions on the mid-shapes, especially for simply supported boundary edges are very limited. The Kirchhoff plate model with isotropic and homogeneous material is studied. The super elliptical powers are chosen from 1 to 10. The Ritz method is employed for the solution of the energy equations of the plates. The effects of Poisson's ratio, which should not be neglected for simply supported plates with curved boundaries, and the aspect ratio of the plate are both examined in detail. The effect of thickness variation is also considered in this study. In order to avoid long computational run times, physically pertinent trial functions are utilized. The frequency parameters obtained are presented and compared with published results for plate shapes that match the current cases.

1. Introduction

Super elliptical plates can be identified with the boundary Eq. (1). Changing the power of the super ellipse, this equation can be used for various geometrical shapes. Although these plates have a broad area of use in mechanical, civil, aerospace and many other engineering branches, they do not have sufficient engineering data as declared by Refs. [1,2]. Considering simply supported curved edges, ignoring the effect of Poisson's ratio, which is in the strain energy expression apart from the one in the bending stiffness of the plate, leads to remarkable error. Therefore, for simply supported boundary conditions, various Poisson's ratio values are employed. Studies on extreme cases of super elliptical plates (circular, elliptical, rectangular) are extensively covered in the literature [3–14]. Yet, the studies on the other shapes that can be expressed by the super elliptical boundary are partial.

Wang et al. [1] obtained solutions for super elliptical plates by using two-dimensional polynomials at a degree of 12 for frequency and buckling factors. Although they worked on diverse super elliptical powers, they

*Corresponding author. Tel.: +35 387 6706 521.
E-mail address: seyit.ceribasi@ucd.ie (S. Çeribaşı).

0022-460X/$ - see front matter
doi:10.1016/j.jsv.2008.06.010

neglected the effect of Poisson's ratio on the behavior of simply supported plates. Altekin [2] studied the static and dynamic behavior of super elliptical plates. He used both variational and weighted residual methods and compared the results, which were obtained in a non-parametrical way. Leissa [3] presented a detailed study on vibration of plates for many plate shapes. Chakraverty et al. [4] studied free vibration of annular elliptical plates through boundary characteristic orthogonal polynomials as trial functions in the Rayleigh–Ritz method. In their work, they considered combinations of simply supported, clamped, and free boundaries for inner and outer edges. They investigated the effect of boundary conditions and hole size on different modes of vibration. Chen et al. [5] employed radial basis function for free vibration analysis of clamped plates and examined the validity of the method by rectangular and circular plates. Enlarging the scope of the works on elliptical plate vibrations to the ones resting on elastic media, Mukherjee [6] obtained the solution of integral equation of the system via orthogonal polynomials.

Despite the huge amount of work on plate vibration, very little has been reported on plates with variable thicknesses. Bayer et al. [7] focused on the vibration of clamped elliptical plates with variable thickness. Solving the equations of the plate by both moment method and Rayleigh–Ritz method, they compared the results for several aspect ratios of the elliptical plates. Vibration of symmetrically laminated super elliptical plates was studied by Chen et al. [8]. Since the transverse shear is an important factor in the mechanical behavior of the laminated composite panels, they preferred shear deformable plate model. Leissa [9], Sato [12], and Narita [13,14] obtained results for simply supported elliptical plates via several methods. Frequency parameters for several values of Poisson's ratios are reported in those studies.

Singh and Tyagi [15] presented results for vibrations of a clamped elliptical plate with variable thickness employing Galerkin's method. Singh and Chakraverty [16] extended the results for elliptical plates to various boundary conditions. They used characteristic orthogonal polynomials satisfying the essential boundary conditions in Ritz method. Zhou et al. [17] and Liew and Feng [18] explored the vibration of super elliptical plates with a three-dimensional approach by using Ritz method.

In the current study, the vibration problem is approached parametrically and the free vibration of super elliptical plates is examined considering sensitivities of the frequency parameters by different super ellipticity degrees, aspect ratios of the super ellipses, Poisson's ratio of the material, and thickness variation. The study is carried out for several Poisson's ratios and plate aspect ratios. Two forms of trial functions are used in the Ritz method; powers of geometrical boundary shape equation and complete sets of polynomials, which are explained in the next section.

2. Basic assumptions and equations

The equation of the boundary for a super ellipse may be expressed as

$$\frac{x^{2n}}{a^{2n}} + \frac{y^{2n}}{b^{2n}} = 1 \tag{1}$$

where n is the power of the super ellipse. The graphical representation of the boundary is as in Fig. 1. In this study the frequency parameters, $\lambda^2 = \omega b^2 \sqrt{\rho h / D}$, are structured according to the geometry presented in this figure.

Selection of the trial functions has crucial importance in accuracy of approximation and is time consuming [19,20]. A trial function for deflection function of the mid-plane, w, may be represented by

$$w = \left(\frac{x^{2n}}{a^{2n}} + \frac{y^{2n}}{b^{2n}} - 1\right)\left(\alpha_{00} + \alpha_{20}\frac{x^2}{a^2} + \alpha_{02}\frac{y^2}{b^2}\right) \tag{2}$$

where α_{00}, α_{20}, and α_{02} are the unknown coefficients. This deflection function possesses such a property that it has the form of two-fold symmetry which is required for the fundamental vibration mode. Although this function gives accurate results for the first vibration mode, it does not give truthful results for higher modes. Also for high powered super ellipses and variable thicknesses the results become very erroneous. Leissa [9] used this shape function for a simply supported ellipse and obtained results for lots of aspect ratios and Poisson's ratios. For convergence studies results of that study are compared with the ones obtained in this study.

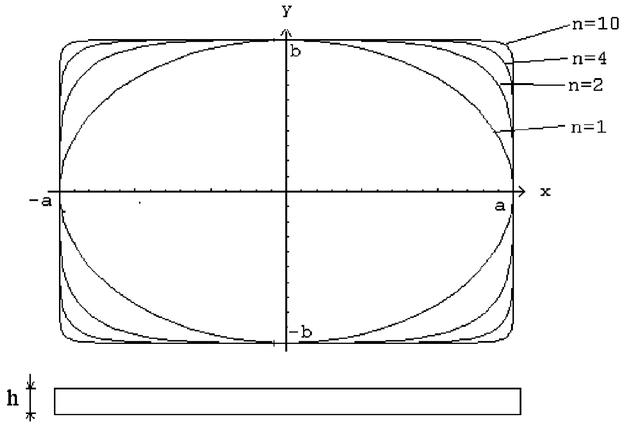

Fig. 1. Super elliptical plate edge in cartesian coordinate system.

Table 1
Shape functions associated with the modes

Plate type	Mode type	Shape function
Homogeneous	Symmetric modes (1,3)	$\alpha_{00}+\alpha_{02}y^2+\alpha_{04}y^4+\alpha_{06}y^6+\alpha_{20}x^2+\alpha_{22}x^2y^2+\alpha_{24}x^2y^4+\alpha_{40}x^4+\alpha_{42}x^4y^2+\alpha_{60}x^6$
Homogeneous	Non-symmetric modes (2)	$\alpha_{00}+\alpha_{01}y^1+\alpha_{02}y^2+\alpha_{03}y^3+\alpha_{10}x^1+\alpha_{11}x^1y^1+\alpha_{12}x^1y^2+\alpha_{20}x^2+\alpha_{21}x^2y^1+\alpha_{30}x^3$
Variable thickness (for $n=1$)	All modes	$\alpha_0+\alpha_1G^1+\alpha_2G^2+\alpha_3G^3+\alpha_4G^4+\alpha_5G^5$ $(G=(x^{2n}/a^{2n}+y^{2n}/b^{2n}-1))$
Variable thickness (for $n=2$, 8)	All modes	$\alpha_{00}+\alpha_{02}y^2+\alpha_{04}y^4+\alpha_{06}y^6+\alpha_{20}x^2+\alpha_{22}x^2y^2+\alpha_{24}x^2y^4+\alpha_{40}x^4+\alpha_{42}x^4y^2+\alpha_{60}x^6$

In this paper, for plates with constant thicknesses complete sets of polynomials as in Eq. (3) are used for deflection functions:

$$w=\left(\frac{x^{2n}}{a^{2n}}+\frac{y^{2n}}{b^{2n}}-1\right)^k[\alpha_{00}x^0y^0+\alpha_{10}x^1y^0+\alpha_{20}x^2y^0+\alpha_{01}x^0y^1+\alpha_{11}x^1y^1+\alpha_{21}x^2y^1+\cdots+\alpha_{ij}x^iy^j] \quad (3)$$

where α_{ij} are unknown coefficients, and k is the power of the geometrical shape equation for satisfying kinematical boundary conditions.

$$k=\left\{\begin{array}{ll}1 & \text{for simply supported boundary conditions}\\ 2 & \text{for clamped boundary conditions}\end{array}\right\}$$

$i+j=p$ is the order of the polynomial. In order to obtain accurate results for the first three modes p values up to 6 are used.

For variable thickness cases, in addition to power series the trial function of Eq. (4) is also used. This function is composed of powers of geometrical boundary shape equation of ellipse, and the boundary conditions are satisfied in the same way of the plates with constant thickness. The shape functions used herein are presented in Table 1

$$w=\left(\frac{x^{2n}}{a^{2n}}+\frac{y^{2n}}{b^{2n}}-1\right)^k\left[\begin{array}{c}\alpha_0+\alpha_1\left(\frac{x^{2n}}{a^{2n}}+\frac{y^{2n}}{b^{2n}}-1\right)^1+\alpha_2\left(\frac{x^{2n}}{a^{2n}}+\frac{y^{2n}}{b^{2n}}-1\right)^2+\alpha_3\left(\frac{x^{2n}}{a^{2n}}+\frac{y^{2n}}{b^{2n}}-1\right)^3\\ +\alpha_4\left(\frac{x^{2n}}{a^{2n}}+\frac{y^{2n}}{b^{2n}}-1\right)^4\end{array}\right] \quad (4)$$

The expression for the strain energy of the plate is

$$U = \frac{1}{2}\iint_A D\left\{\left(\frac{\partial^2 w}{\partial x^2}+\frac{\partial^2 w}{\partial y^2}\right)^2 - 2(1-\nu)\left[\frac{\partial^2 w}{\partial x^2}\frac{\partial^2 w}{\partial y^2}-\left(\frac{\partial^2 w}{\partial x \partial y}\right)^2\right]\right\} \mathrm{d}x\,\mathrm{d}y \tag{5}$$

where $D = Eh^3/[12(1-\nu^2)]$ is the bending rigidity, E is Young's modulus, and ν is Poisson's ratio. Although increasing more powers of boundary equation in Eq. (4) gives more accurate results, this causes excessive run time and requires very high computer memory which is not available in current market computers, except special designed ones.

The expression representing the kinetic energy of the plate is

$$T = \frac{1}{2}\iint_A \rho h(x,y)\left[\frac{\partial w(x,y,t)}{\partial t}\right]^2 \mathrm{d}x\,\mathrm{d}y \tag{6}$$

Assuming that the plate is undergoing harmonic oscillations the deflection can be written as

$$w(x,y,t) = W(x,y)\sin(\omega t) \tag{7}$$

where $W(x, y)$ is the trial function and ω represents the unknown natural circular frequency of the plate pertinent to the assumed shape function. Substituting Eq. (7) into the expression of the kinetic energy of the oscillating plate a new expression for kinetic energy can be obtained as

$$T = \frac{\omega^2}{2}\cos^2(\omega t)\iint_A \rho h(x,y) W^2(x,y)\,\mathrm{d}x\,\mathrm{d}y \tag{8}$$

The kinetic energy is at the maximum level when the velocity of the plate is maximum which occurs when $w(x, y, t)$ is zero. This is the case when $\sin(\omega t)$ is zero, which means:

$$\omega t = n\pi \quad (n = 0, 1, 2, \ldots) \tag{9}$$

Substituting the last expression into Eq. (8), the maximum kinetic energy expression becomes:

$$T = \frac{\omega^2}{2}\iint_A \rho h(x,y) W^2(x,y)\,\mathrm{d}x\,\mathrm{d}y \tag{10}$$

The strain energy is maximum when the deflection of the plate is maximum. This occurs when $\sin(\omega t)$ equals to 1. Using these values of ωt the expression of maximum strain energy becomes identical to Eq. (5).

In order to apply the Ritz method firstly an appropriate deflection shape is selected, which is Eq. (4), and then maximum kinetic and strain energies are equated. An equation in the following form is obtained:

$$\begin{aligned}\Pi = {} & \frac{1}{2}\iint_A D\left\{\left(\frac{\partial^2 W}{\partial x^2}+\frac{\partial^2 W}{\partial y^2}\right)^2 - 2(1-\nu)\left[\frac{\partial^2 W}{\partial x^2}\frac{\partial^2 W}{\partial y^2}-\left(\frac{\partial^2 W}{\partial x \partial y}\right)^2\right]\right\} \mathrm{d}x\,\mathrm{d}y \\ & -\frac{\omega^2}{2}\iint_A \rho h(x,y) W^2(x,y)\,\mathrm{d}x\,\mathrm{d}y = 0\end{aligned} \tag{11}$$

In this study Eq. (11) is solved by Ritz method.

If all of the edges of the plate are fixed, the second term on the right-hand side of the first integral expression becomes zero. Therefore the effect of Poisson's ratio vanishes. The same situation also holds for straight edged plates. Thus the expression for total potential energy takes the form:

$$\Pi = \frac{1}{2}\iint_A D\left\{\left(\frac{\partial^2 W}{\partial x^2}+\frac{\partial^2 W}{\partial y^2}\right)^2\right\} \mathrm{d}x\,\mathrm{d}y - \frac{\omega^2}{2}\iint_A \rho h(x,y) W^2(x,y)\,\mathrm{d}x\,\mathrm{d}y = 0 \tag{12}$$

3. Plates with variable thickness

In this part of the current study a parabolic variation of the plate thickness in structure of Eq. (13) is assumed:

$$h(x,y) = ch_0[\alpha + \beta(x^2 + y^2)] \tag{13}$$

$$c = \frac{2}{(2\alpha + \beta)} \tag{14}$$

where α and β are parameters designating non-homogeneity. In Eqs. (13) and (14) h_0 is the constant thickness of the plate, α is the parameter which defines the constant part of the plate, β is the parameter which controls the variation of the thickness, and c is a parameter which controls the volumes of the plates.

In case of thickness variation the bending rigidity also varies and takes the form:

$$D(x,y) = D_0 c^3 H \tag{15}$$

In Eq. (15) $D_0 = Eh^3/[12(1-v^2)]$ is the bending rigidity of the plate with constant thickness and,

$$H = [\alpha + \beta(x^2 + y^2)]^3 \tag{16}$$

After substituting Eqs. (13) and (15) into Eq. (11) the potential energy equation gets the form:

$$\Pi = \frac{1}{2}\iint_A D_0 c^3[\alpha + \beta(x^2 + y^2)]^3 \left\{ \left(\frac{\partial^2 W}{\partial x^2} + \frac{\partial^2 W}{\partial y^2}\right)^2 - 2(1-v)\left[\frac{\partial^2 W}{\partial x^2}\frac{\partial^2 W}{\partial y^2} - \left(\frac{\partial^2 W}{\partial x \partial y}\right)^2\right]\right\} \mathrm{d}x\,\mathrm{d}y - \frac{\omega^2}{2}\iint_A \rho c h_0[\alpha + \beta(x^2 + y^2)] W^2(x,y)\,\mathrm{d}x\,\mathrm{d}y = 0 \tag{17}$$

4. Solution by the Ritz method

The objective of the variational methods is to find from a group of admissible functions those which represent the deflections of the elastic body, pertinent to its stable equilibrium conditions. The essence of the Ritz method is the application of principle of minimum potential energy.

The principle of minimum potential energy makes use of the change of the total potential during arbitrary variation of the deflection. Introducing δu, δv, and δw as the virtual displacements of the elastic body, the new position ($u+\delta u$, $v+\delta v$, $w+\delta w$) produces an increase in the strain energy stored. The change in the total potential energy can be evaluated as

$$\delta\Pi = \Pi(u + \delta u,\ v + \delta v,\ w + \delta w) - \Pi(u, v, w) \tag{18}$$

Since the equilibrium configuration is represented by those admissible functions which make the total potential of the system minimum, it can be stated that,

$$\delta\Pi = \delta U + \delta V = \delta(U + V) = 0 \tag{19}$$

Components of the compatible infinitesimal virtual displacements (δu, δv, δw) should satisfy the geometrical boundary conditions of the elastic system, and be capable of representing all possible displacement patterns. If these admissible displacement functions are chosen properly very good accuracy can be attained.

The deflected middle surface of a plate can be represented in the form of a series:

$$w(x,y) = \alpha_1 f_1(x,y) + \alpha_2 f_2(x,y) + \alpha_3 f_3(x,y) + \cdots + \alpha_n f_n(x,y) = \sum_{i=1}^{p} \alpha_i f_i(x,y) \tag{20}$$

where $f_i(x, y)$, ($i = 1, 2, 3, \ldots, p$), are continuous functions that satisfy individually at least the geometrical boundary conditions and are capable of representing the deflected plate surface. The functions used herein are two-dimensional and in the form of

$$f_{i,j}(x,y) = \left(\frac{x^{2n}}{a^{2n}} + \frac{y^{2n}}{b^{2n}} - 1\right)^k x^i y^j \tag{21}$$

The unknown constants $\alpha_1, \alpha_2, \alpha_3, \ldots, \alpha_n$ are determined from the minimum potential energy principle as

$$\frac{\partial \Pi}{\partial \alpha_1} = 0, \frac{\partial \Pi}{\partial \alpha_2} = 0, \ldots, \frac{\partial \Pi}{\partial \alpha_n} = 0 \tag{22}$$

Table 2
The calculated perimeter and area of the super ellipses for $a = 1$ and $b = 1$

n	Perimeter	Area
1	6.2832	3.1416
2	7.0177	3.4961
3	7.3178	3.6430
4	7.4798	3.7235
5	7.5814	3.7744
6	7.6510	3.8094
7	7.6932	3.8350
8	7.7374	3.8546
9	7.7635	3.8700
10	7.7809	3.8824

Table 3
Convergence of results with increasing terms

Shape function	Clamped		Simply supported	
	λ_1^2	λ_3^2	λ_1^2	λ_3^2
α_{00}	12.5959	–	9.2448	–
$\alpha_{00}+\alpha_{20}x^2$			7.6033	44.7247
$\alpha_{00}+\alpha_{20}x^2+\alpha_{02}y^2$	10.1053	40.0440	5.1284	44.1744
$\alpha_{00}+\alpha_{20}x^2+\alpha_{02}y^2+\alpha_{22}x^2y^2$	9.8171	39.9858	5.1025	44.1737
$\alpha_{00}+\alpha_{20}x^2+\alpha_{02}y^2+\alpha_{22}x^2y^2+\alpha_{40}x^4$	9.1205	34.8224	4.8731	27.2449
$\alpha_{00}+\alpha_{20}x^2+\alpha_{02}y^2+\alpha_{22}x^2y^2+\alpha_{40}x^4+\alpha_{04}y^4$	8.6289	34.8223	4.8182	26.6303
$\alpha_{00}+\alpha_{02}y^2+\alpha_{04}y^4+\alpha_{06}y^6+\alpha_{20}x^2+\alpha_{22}x^2y^2+\alpha_{24}x^2y^4+\alpha_{40}x^4+\alpha_{42}x^4y^2+\alpha_{60}x^6$	8.6017	30.4910	4.7359	26.6121

Table 4
Comparison of the frequency parameters ($\lambda^2 = \omega b^2\sqrt{\rho h/D}$) with previously obtained results

n		v	$a/b = 1$	$a/b = 1.5$	$a/b = 2$	$a/b = 3$
1	Present	0.3	4.935	3.687	3.314	3.035
1	Wang et al. [1]	–	4.935	3.681	3.303	3.009
1	Sato [12]	0.3	4.935	–	3.293	–
1	Narita [13]	0.3	4.935	–	3.303	–
1	Prakash and Ganapathi [21]	–	4.935	–	–	–
8	Present	0.3	5.066	3.775	3.15	2.783
8	Wang et al. [1]	–	4.804	3.486	3.038	2.723

With this minimization procedure n simultaneous algebraic equations, in terms of the unknown coefficients, are obtained. The number of the equations is equal to the number of the unknown coefficients, so $\alpha_1, \alpha_2, \alpha_3, \ldots, \alpha_n$ can be calculated.

Table 5
Comparison of the fundamental mode, $\lambda^2 = \omega b^2\sqrt{\rho h/D}$, with Leissa [9] and Singh and Chakraverty [22]

a/b	$v = 0.25$			$v = 0.5$		
	Present	Leissa	Singh	Present	Leissa	Singh
1.0	4.8601	4.865	4.8601	5.2127	5.219	5.2127
1.1	4.4490	4.454	4.4489	4.7662	4.772	4.7662
1.2	4.1526	4.157	4.1526	4.4356	4.442	4.4356
1.4	3.7679	3.773	3.7679	3.9898	3.990	3.9898
1.7	3.4555	3.463	3.4555	3.6078	3.617	3.6078
2.0	3.2813	3.292	3.2813	3.3866	3.399	3.3866
2.5	3.1098	3.128	3.1098	3.1698	3.189	3.1698
3.0	3.0014	3.027	3.0014	3.0387	3.066	3.0387

Table 6
Frequency parameters, $\lambda^2 = \omega b^2\sqrt{\rho h/D}$, for simply supported super elliptical plates with constant thickness

n	a/b	λ_1^2			λ_2^2			λ_3^2		
		$v = 0.1$	$v = 0.2$	$v = 0.3$	$v = 0.1$	$v = 0.2$	$v = 0.3$	$v = 0.1$	$v = 0.2$	$v = 0.3$
1	1.0	4.6192	4.7826	4.9351	13.7208	13.8564	13.8985	25.3757	25.4988	25.6188
	1.2	3.9596	4.0904	4.2128	10.4107	10.5377	10.5909	19.6477	19.765	19.8787
	1.4	3.6173	3.7193	3.8149	8.4587	8.5730	8.6210	15.4489	15.5607	15.6686
	1.6	3.4213	3.5002	3.5743	7.2280	7.3277	7.3626	12.6742	12.7777	12.8768
	2.0	3.2114	3.2586	3.3034	5.8399	5.9107	5.9105	9.4287	9.5108	9.5886
	3.0	2.9779	2.9937	3.0090	4.5181	4.5442	4.4578	6.2711	6.3060	6.3389
	4.0	2.8549	2.8624	2.8699	4.0136	4.0254	3.8735	5.1026	5.1170	5.1309
2	1.0	4.6072	4.6497	4.7359	12.8983	13.0182	13.2215	26.4938	26.5625	26.6121
	1.2	3.9515	4.0238	4.0928	9.6163	9.7290	9.8387	20.4277	20.5440	20.6572
	1.4	3.5509	3.6125	3.6712	7.6853	7.7897	7.8910	16.0930	16.2181	16.3407
	1.6	3.3029	3.3562	3.4067	6.4708	6.5663	6.6587	13.3160	13.4366	13.5551
	2.0	3.0292	3.0699	3.1084	5.1167	5.1947	5.2698	10.2047	10.3081	10.4098
	3.0	2.7929	2.8149	2.8358	3.9375	3.9824	4.0254	7.5246	7.5885	7.6513
	4.0	2.7244	2.7371	2.7492	3.5909	3.6172	3.6425	6.7668	6.8087	6.8497
8	1.0	5.0624	5.0640	5.0655	14.7895	14.7918	14.7932	28.5913	28.6078	28.6231
	1.2	4.2876	4.2891	4.2904	11.1777	11.1855	11.1921	21.9232	21.9335	21.9421
	1.4	3.8182	3.8196	3.8209	8.9294	8.9401	8.9496	17.3429	17.3613	17.3777
	1.6	3.5114	3.5129	3.5143	7.4424	7.4545	7.4654	14.2673	14.2902	14.3110
	2.0	3.1463	3.1480	3.1496	5.6701	5.6826	5.6941	10.5228	10.5429	10.5613
	3.0	2.7802	2.7818	2.7832	3.9154	3.9237	3.9315	6.5720	6.5741	6.5759
	4.0	2.6531	2.6541	2.6551	3.3168	3.3210	3.3249	5.0486	5.0467	5.0448
10	1.0	5.1800	5.1805	5.181	15.4827	15.4827	15.4828	30.2072	30.2202	30.2322
	1.2	4.3874	4.3879	4.3883	11.6837	11.6894	11.6943	23.4866	23.4993	23.5105
	1.4	3.9071	3.9076	3.9080	9.3292	9.3380	9.3458	18.6763	18.6975	18.7168
	1.6	3.5924	3.5929	3.5933	7.7761	7.7863	7.7956	15.3855	15.4102	15.4328
	2.0	3.2144	3.2151	3.2158	5.9221	5.9324	5.9419	11.3243	11.3433	11.3608
	3.0	2.8239	2.8249	2.8259	4.0659	4.0721	4.0779	7.0104	7.0110	7.0114
	4.0	2.6844	2.6851	2.6859	3.4294	3.4324	3.4352	5.3628	5.361	5.3593

Table 7
Frequency parameters, $\lambda^2 = \omega b^2\sqrt{\rho h/D}$, for clamped super elliptical plates with constant thickness

n	a/b	λ_1^2	λ_2^2	λ_3^2
1	1.0	10.2158	21.2749	34.9408
	1.2	8.7178	16.4582	27.2553
	1.4	7.8910	13.6449	21.7666
	1.6	7.3928	11.8820	18.1925
	2.0	6.8444	9.8985	14.0819
	3.0	6.3119	8.0331	10.2272
	4.0	6.1037	7.3889	8.9518
2	1.0	8.6017	19.6330	30.4910
	1.2	7.8785	14.9489	25.6566
	1.4	7.1584	12.2512	20.0958
	1.6	6.7265	10.5966	16.6119
	2.0	6.2536	8.8143	12.7718
	3.0	5.8060	7.3198	9.5366
	4.0	5.6468	6.8561	8.5455
8	1.0	9.3005	26.7632	44.5642
	1.2	7.9395	19.2351	34.4356
	1.4	7.1935	15.3328	27.7945
	1.6	6.7495	12.7312	23.2008
	2.0	6.2766	7.3449	17.4107
	3.0	5.8716	7.0101	11.3081
	4.0	5.7483	6.2872	9.1652
10	1.0	9.3763	27.6621	48.9207
	1.2	8.0022	20.8522	38.0785
	1.4	7.2459	16.5062	30.8002
	1.6	6.7934	13.6137	25.6814
	2.0	6.3068	10.2140	19.1815
	3.0	5.8826	7.1564	12.3145
	4.0	5.7520	6.3285	9.9107

5. Integration over the super elliptical region

During solutions of differential equations with approximate methods there are difficulties arising from integration over a super elliptical area. Any deviation from the area of the super ellipse causes extra error in the results. Calculating the area and perimeter of the region may give an idea about the convergence of the integration. Therefore the areas and perimeters of the super ellipses are calculated for $a = 1$ and $b = 1$. If $a = 1$ and $b = 1$ then the super elliptical function becomes:

$$x^{2n} + y^{2n} - 1 = 0 \tag{23}$$

$$y = \sqrt[2]{1 - x^{2n}} \tag{24}$$

and

$$y' = -x^{-1+2n}(1 - x^{2n})^{-1+1/2n} \tag{25}$$

Thus, calculation of the Riemann sum as

$$s \approx \sum_{i=1}^{n} \sqrt{1 + y'^2}\,\Delta x \tag{26}$$

gives the length of any curve. In that case the exact value of the perimeter should be expected for $n = 1$.

The shapes of the super ellipses for $n = 1$ and 10 are a circle with a radius of 1 and a shape close to a square with an edge length of 2, respectively. The results obtained are as expected and are shown in Table 2.

6. Presentation of the results

Circles and ellipses are special cases of super elliptical forms which were studied previously. In Table 3 convergence of results with increasing polynomial terms is presented and some results of the numerical analysis are compared with references' results in Table 4. The results obtained by the references were presented in different parametric forms. In order to make comparison, all values are transformed to the parameter $\omega b^2\sqrt{\rho h/D}$, which is used in the entire study. Some of the frequency parameter values differ from our results. This variation results from use of different solution methods and different trial functions.

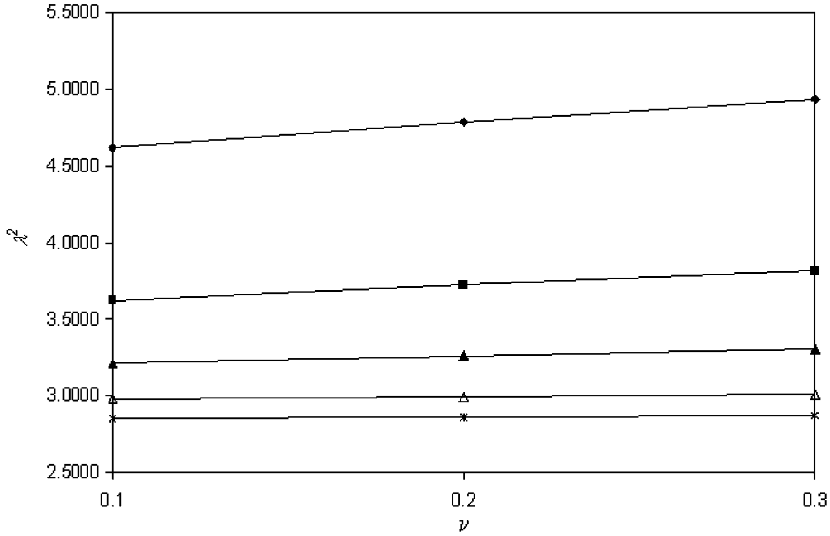

Fig. 2. Change of the fundamental frequency parameter λ^2 of a simply supported elliptical plate with respect to ν ((—◆—) $a/b = 1$, (—■—) $a/b = 1.4$, (—▲—) $a/b = 2$, (—△—) $a/b = 3$, (—✱—) $a/b = 4$).

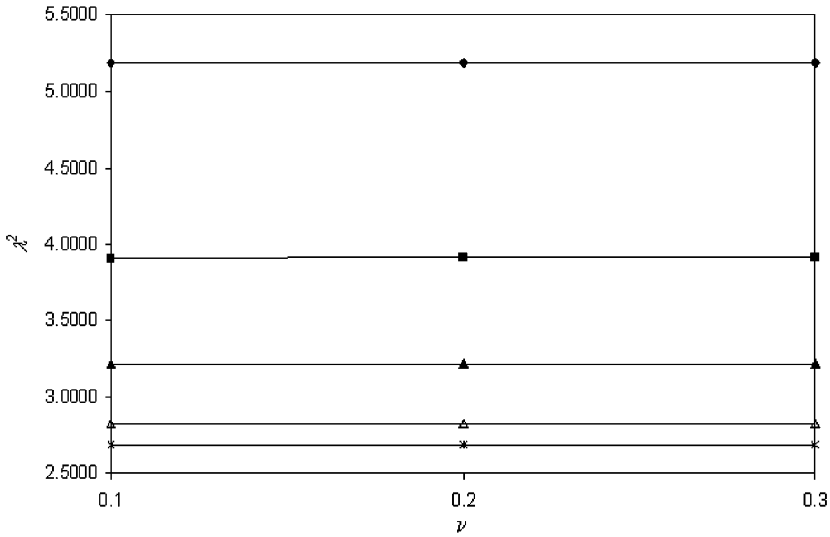

Fig. 3. Change of the fundamental frequency parameter λ^2 of a simply supported super elliptical plate of $n = 10$ with respect to ν ((—◆—) $a/b = 1$, (—■—) $a/b = 1.4$, (—▲—) $a/b = 2$, (—△—) $a/b = 3$, (—✱—) $a/b = 4$).

The results for ellipses are widely reported in the literature; therefore elliptical shapes are very convenient for benchmarking purposes. We carried out computations for 8 aspect ratios with $v = 0.25$ and 0.5 for the fundamental mode to compare our results with Leissa [9] and Singh and Chakraverty [22]. In Table 5 these results are presented and good agreement is attained with their results.

In Table 6 frequency parameters for first 3 modes of 4 types of simply supported super elliptical plates with v values of 0.1, 0.2 and 0.3 are reported. It is clear that as v is increased the frequency parameters also increase and with increasing a/b ratios the parameters decrease. At high a/b ratios the effect of v decreases and also the parameters of different super ellipses becomes very similar. These results are valid for all of the 3 modes. The

Table 8
Frequency parameters, $\lambda^2 = \omega b^2 \sqrt{\rho h_0 / D_0}$, for clamped super elliptical plates with variable thickness

n	β	α	a/b				
			1.0			0.8	0.2
			λ_1^2	λ_2^2	λ_3^2	λ_1^2	λ_1^2
1	0.0	1.0	10.2158	39.8372	86.7407	13.2458	158.5923
1		Ref. [3]	10.216			13.229	149.89
1		Ref. [15]	10.216	39.771	89.106	13.246	158.59
1							
2		1.0	8.6108	33.4003	84.6464	11.1457	130.9290
8		1.0	9.3005	–	–	12.3501	143.1174
1	0.1	0.1	10.42737	36.1421	82.0731	13.6150	175.7097
1		Ref. [16]	10.6	–	–	13.61	150.3
1	0.4	1.0	10.3613	38.2207	85.3728	13.4789	167.4870
1		0.6	10.4036	37.2419	83.5732	13.5582	171.6945
1		0.4	10.4247	36.1421	82.0731	13.6116	175.7159
1		0.0	13.9764	37.5610	101.5613	18.4298	269.8621
8	0.4	1.0	16.3514	–	–	13.8841	151.2620
8		0.6	18.4617	–	–	14.9147	154.9988
8		0.4	20.8206	–	–	16.2125	158.7762
8		0.0	51.5213	–	–	46.5247	331.3280
1	0.6	1.0	10.3957	37.4793	83.9681	13.5422	170.7398
1		0.6	10.4247	36.1421	82.0731	13.6116	175.7159
1		0.4	10.4221	34.7856	80.9284	13.6396	180.0826
1		0.0	13.9764	37.5609	101.5610	18.4298	269.8621
8	0.6	1.0	17.9529	–	–	14.6560	154.1450
8		0.6	20.8206	–	–	16.2125	158.7762
8		0.4	23.8357	–	–	18.1247	163.7357
8		0.0	51.5213	–	–	46.5247	331.3280
1	1.0	1.0	10.4247	36.1421	82.0731	13.6116	175.7159
1		0.6	10.4166	34.4098	80.7475	13.6413	181.2419
1		0.4	10.3805	33.0136	80.6734	13.6299	185.7919
1		0.0	13.9764	37.5610	101.5613	18.4298	269.8621
2	1.0	1.0	10.5981	37.7942	83.9800	12.0460	154.1212
2		0.6	11.6319	40.3050	92.1581	12.4485	164.1702
2		0.4	12.7057	42.8516	99.2933	12.9148	174.0754
2		0.0	21.6957	62.1708	135.4570	20.4829	282.0777
8	1.0	1.0	20.8206	–	–	16.2125	158.7762
8		0.6	24.7201	–	–	18.7402	165.3285
8		0.4	28.4311	–	–	21.5802	173.2132
8		0.0	51.5213	–	–	46.5247	331.3280

parameters for clamped boundary conditions are presented in Table 7. The variation of frequency parameters of clamped plates is v independent. The effect of aspect ratio is the same as the effect on the simply supported plates.

Table 9
Frequency parameters, $\lambda^2 = \omega b^2 \sqrt{\rho h_0 / D_0}$, for simply supported super elliptical plates with variable thickness

n	β	α	a/b				
			1.0			0.8	0.2
			λ_1^2	λ_2^2	λ_3^2	λ_1^2	λ_1^2
1	0.0	1.0	4.9351	29.7201	74.6830	6.4034	77.2922
2		1.0	4.7359	25.3307	76.2596	5.8880	65.8396
8		1.0	5.0655	–	–	6.8048	63.2498
1	0.1	0.1	4.5605	26.33179	70.83201	5.9143	70.9674
1	Ref. [16]	0.1	5.035	–	–	6.535	70.31
1	0.4	1.0	4.7207	28.14752	72.16911	6.1239	73.7418
1		0.6	4.6311	27.2604	71.3105	6.0068	72.2154
1		0.4	4.5605	26.3318	70.83201	5.9143	70.9680
1		0.0	5.8754	28.3969	94.6047	7.6108	90.0799
2	0.4	1.0	4.6039	27.6610	71.7065	5.8605	62.2229
2		0.6	4.6744	28.5688	75.7998	5.8903	60.6093
2		0.4	4.7909	29.6924	79.9329	5.9603	59.2548
2		0.0	7.9663	52.2200	117.1394	9.3806	74.9330
8	0.4	1.0	7.1977	–	–	7.5553	55.5622
8		0.6	7.9595	–	–	8.1161	51.4971
8		0.4	8.8424	–	–	8.7974	47.3216
8		0.0	20.7296	–	–	18.4471	27.3551
1	0.6	1.0	4.6503	27.4698	71.4777	6.0319	72.5464
1		0.6	4.5605	26.3318	70.83201	5.9143	70.9680
1		0.4	4.5120	25.26604	70.8382	5.8502	70.0237
1		0.0	5.8754	28.3969	94.6047	7.6108	90.0799
2	0.6	1.0	4.6543	28.3409	74.8562	5.8801	60.9627
2		0.6	4.7909	29.6924	79.9329	5.9603	59.2548
2		0.4	4.9890	31.2671	84.7721	6.1020	58.1826
2		0.0	7.9663	52.2200	117.1394	9.3806	74.9330
8	0.6	1.0	7.7729	–	–	7.9758	52.4464
8		0.6	8.8424	–	–	8.7974	47.3216
8		0.4	9.9995	–	–	9.7161	42.4853
8		0.0	20.7296	–	–	18.4471	27.3551
1	1.0	1.0	4.5605	26.3318	70.83201	5.9143	70.9680
1		0.6	4.5063	24.9839	70.9535	5.8424	69.8799
1		0.4	4.5229	23.9774	71.9113	5.8626	69.9169
1		0.0	5.8754	28.3969	94.6047	7.6108	90.0799
2	1.0	1.0	4.7909	29.6924	79.9329	5.9603	59.2548
2		0.6	5.0561	31.7547	86.1163	6.1542	58.0050
2		0.4	5.3733	33.9143	91.4499	6.4217	57.9146
2		0.0	7.9663	52.2200	117.1394	9.3806	74.9330
8	1.0	1.0	8.8424	–	–	8.7974	47.3216
8		0.6	10.3427	–	–	9.9917	41.1701
8		0.4	11.7927	–	–	11.1645	36.1786
8		0.0	20.7296	–	–	18.4471	27.3551

For the round edged simply supported plates Poisson's ratio-dependent term should not be neglected. In Figs. 2 and 3, the effect of Poisson's ratio on low and high ordered super ellipses is accentuated. The changes of the fundamental frequencies with respect to Poisson's ratio are compared. It is seen that the Poisson's ratio effect becomes very minimal when high values of n are used for the super elliptical boundary shape equation. In Fig. 2 elliptical shapes are considered and there are noticeable changes with changing Poisson's ratios especially for low aspect ratios. In Fig. 3 super ellipses geometrically similar to rectangles are considered and the lines which represent the trend of the change are horizontal which means that the effect of Poisson's ratio is negligible for high powered super ellipses.

In context of this study the outcome of thickness variation is also considered. This effect is governed by 2 more parameters than the constant thickness cases, which are the controlling parameter of constant part of the plate (α) and controlling parameter of the thickness variation (β). Results of variable thickness calculations are obtained for Poisson's ratio of 0.3. The parameters for clamped and simply supported cases are presented in Tables 8 and 9, respectively. Because of many controlling parameters the amount of probable combinations is quite large. For some coinciding combinations comparisons with results from literature are also presented in the same tables.

7. Concluding remarks

In Tables 6 and 7 the frequency parameters, λ^2, for 3 modes of super elliptical plates with constant thickness are tabulated for different values of a/b ratios and Poisson's ratios. Considering super ellipticity levels, the v dependency is significant for low n values, but for high values of n where the plate edges are very straight there is almost no v dependency. In Figs. 2 and 3, the v dependency of the frequency parameters is examined in a graphical form for $n = 1$ and 10, respectively, in order to see the variation of the parameters for different super ellipticity levels. For elliptical shapes with $a/b = 1$ the ratio of λ^2 for $v = 0.3$ to the one for $v = 0.1$ is 1.0684, whereas the same ratio for $n = 10$ is 1.0002. From Fig. 2 the dependency of the frequency parameters can also be examined for changing a/b values. It is clearly seen that for high $a/$b ratios the v dependency is negligible because the slopes of the lines for these ratios are close to 0.

For super elliptical plates with variable thickness one can make the following observations from the results given in Tables 8 and 9. For clamped plates if all the other parameters are kept fixed then the frequency parameters increase with decreasing α values and this increase amount is sharp when α gets close to 0. If β parameter is varied the change in frequency parameters is very small and the direction of the change of frequency parameters is the same as the direction of the change of β. For simply supported plates the observed change with respect to α is very small except for $\alpha = 0$. When $\alpha = 0$ the same sharp change is observed.

References

[1] C.M. Wang, L. Wang, K.M. Liew, Vibration and buckling of super elliptical plates, *Journal of Sound and Vibration* 171 (3) (1994) 301–314.

[2] M. Altekin, Static and Dynamic Analysis of Super-Elliptical Plates, Ph.D. Thesis, Bogazici University, 2005.

[3] A.W. Leissa, *Vibration of Plates-NASA SP-160*, US Government Printing Office, Washington, DC, 1969.

[4] S. Chakraverty, R.B. Bhat, I. Stiharu, Free vibration of annular elliptic plates using boundary characteristic orthogonal polynomials as shape functions in the Rayleigh–Ritz method, *Journal of Sound and Vibration* 241 (3) (2001) 524–539.

[5] J.T. Chen, I.L. Chen, K.H. Chen, Y.T. Lee, Y.T. Yeh, A meshless method for free vibration analysis of circular and rectangular clamped plates using radial basis function, *Engineering Analysis with Boundary Elements* 28 (2004) 534–545.

[6] M. Mukherjee, Forced vertical vibrations of an elastic elliptic plate on an elastic half space—a direct approach using orthogonal polynomials, *International Journal of Solids and Structures* 38 (2001) 389–399.

[7] I. Bayer, U. Güven, G. Altay, A parametric study on vibrating clamped elliptical plates with variable thickness, *Journal of Sound and Vibration* 254 (1) (2002) 179–188.

[8] C.C. Chen, C.W. Lim, S. Kitipornchai, K.M. Liew, Vibration of symmetrically laminated thick super elliptical plates, *Journal of Sound and Vibration* 220 (4) (1999) 659–682.

[9] A.W. Leissa, Vibration of a simply-supported elliptical plate, *Journal of Sound and Vibration* 6 (1) (1967) 145–148.

[10] R. Szillard, *Theory and Analysis of Plates: Classical and Numerical Methods*, Prentice-Hall, Englewood Cliffs, NJ, 1974.

[11] I.H. Shames, C.L. Dym, *Energy and Finite Element Methods in Structural Mechanics*, Hemisphere, Washington, DC, 1991.

[12] K. Sato, Free flexural vibrations of an elliptical plate with simply supported edge, *Journal of the Acoustical Society of America* 52 (1972) 919–922.
[13] Y. Narita, Natural frequencies of free, orthotropic elliptical plates, *Journal of Sound and Vibration* 100 (1) (1985) 83–89.
[14] Y. Narita, Free vibration analysis of orthotropic elliptical plates resting on arbitrarily distributed point supports, *Journal of Sound and Vibration* 108 (1) (1986) 1–10.
[15] B. Singh, D.K. Tyagi, Transverse vibrations of an elliptical plate with variable thickness, *Journal of Sound and Vibration* 99 (3) (1985) 379–391.
[16] B. Singh, S. Chakraverty, Use of characteristic orthogonal polynomials in two dimensions for transverse vibration of elliptic and circular plates with variable thickness, *Journal of Sound and Vibration* 173 (3) (1994) 289–299.
[17] D. Zhou, S.H. Lo, Y.K. Cheung, F.T.K. Au, 3-D vibration analysis of generalized super elliptical plates using Chebyshev–Ritz method, *International Journal of Solids and Structures* 41 (2004) 4697–4712.
[18] K.M. Liew, Z.C. Feng, Three-dimensional free vibration analysis of perforated super elliptical plates via the p-Ritz method, *International Journal of Mechanical Sciences* 43 (2001) 2613–2630.
[19] V.N. Kaliakin, *Introduction to Approximate Solution Techniques, Numerical Modeling, and Finite Element Methods*, Marcel Dekker, New York, 2002.
[20] O. Shisha, Trends in approximation theory, *Applied Mechanics Reviews* 21 (4) (1968) 337–341.
[21] T. Prakash, M. Ganapathi, Asymmetric vibration and thermoelastic stability of FGM circular plates using finite element method, *Composites: Part B* 37 (2006) 642–649.
[22] B. Singh, S. Chakraverty, Transverse vibration of simply supported elliptical and circular plates using boundary characteristic orthogonal polynomials in two variables, *Journal of Sound and Vibration* 152 (1) (1992) 149–155.